Supplementary Information

Deconstructing Culture Media Reveals a Key Role of Oxyanion Salts on the Physicochemical Properties of *Ortho*-Aminomethyl-Phenylboronic Acid/Glucamine hydrogels in Aqueous Environments

Léa Terriac[1], Khaled Alsabi[2], Elise Patingre[1], Ewen Tertrin[1], Yves Maugars[1], Catherine Garnier[3], Jean-Jacques Helesbeux[2], Vianney Delplace[1]

[1] INSERM Regenerative Medecine and Skeleton RMeS, Univ. Nantes, Nantes, France

[2] Univ Angers, SONAS, SFR QUASAV, F-49000 Angers, France

[3] INRAE, UR 1268 BIA Biopolymères Interactions Assemblages, Nantes, France

Association constant calculation

As previously described in the literature, the association constant of PBA-diol complexes can be calculated by titrating a PBA-Alizarin Red (ARS) solution with the diol of interest.[1,2] In this method, the first step is the determination of the PBA-ARS association constant. To do so, solutions were prepared with constant concentration in ARS (0.15 mM in phosphate buffer, PBS) and a range of concentrations for PBA (1 to 35 mM in phosphate buffer, PBS, depending on the PBA). A solution with ARS at 0.15 mM and without PBA was kept as a reference for the following calculations. All the solutions were buffered to pH 7.4. The maximum of absorbance of the free ARS molecule is around 530 nm, upon complexation with PBA, the color of the solutions shifted from pink to yellow, the maximum of absorbance of the PBA-ARS complex is around 450 nm. Depending on the experiment, the absorbance of either the free ARS molecule (λ = 530 nm) or the PBA-ARS complex (λ = 450 nm) was used to obtain the most accurate result. All the absorbances were measured on 96-well plates with a Tristar 2 from Berthold Technologies. To calculate the association constant, several equations were used as described below:

$$K_{ARS} = \frac{[PBA - ARS]}{[PBA][ARS]} \quad \textbf{(1)}$$

$$[ARS] = [ARS]_0 - [PBA - ARS] \quad \textbf{(2)}$$

From **(1)** and **(2):**

$$K_{ARS} = \frac{[PBA - ARS]}{[PBA]([ARS]_0 - [PBA - ARS])} \quad \textbf{(3)}$$

(3) can also be written as:

$$\frac{[ARS]_0}{[PBA - ARS]} = \frac{1}{[PBA]K_{ARS}} + 1 \quad \textbf{(4)}$$

From Beer-Lambert law, the absorbance at 530 nm is equal to A = k.$[ARS]$, were k is a constant, then

$\Delta A = A_{ARS} - A_{PBA\text{-}ARS\ sample} = k.[ARS]_0 - k.[ARS] = k.([ARS]_0 - [ARS]) = k.[PBA - ARS]$ **(5)**

From Beer-Lambert law, the absorbance at 450 nm is equal to A = k.$[PBA - ARS]$, where k is a constant, then

$$\Delta A = A_{PBA\text{-}ARS\ sample} - A_{ARS} = k.[ARS] - k.[ARS]_0 = k.[PBA - ARS] \quad \textbf{(5bis)}$$

From **(4)** and **(5)** or **(5bis):**

$$\frac{k.[ARS]_0}{\Delta A} = \frac{1}{[PBA]K_{ARS}} + 1 \quad \textbf{(6)}$$

(6) can also be written as:

$$\frac{1}{\Delta A} = \frac{1}{[PBA]K_{ARS}.k.[ARS]_0} + \frac{1}{k.[ARS]_0} \quad \textbf{(7)}$$

As $[PBA]_0 \gg [ARS]_0$, we assumed that $[PBA]_0 \approx [PBA]$. Absorbance of all the solutions that cover a range of adapted for each PBA (between 1 mM to 35 mM mixed with 0.15 mM of ARS) was measured at 530 nm. $\frac{1}{\Delta A}$ was calculated with ΔA equal to the absorbance of the pure ARS solution minus the absorbance of the given solution of the PBA range. $\frac{1}{\Delta A}$ was plotted in function of $\frac{1}{[PBA]_0}$. From the linear regression, the slope and the plot intercept can be extracted. The K_{ARS} is the result of the division of the plot intercept by the slope.

The second step is the determination of the PBA-diol association constant. To do so, solutions were prepared with constant concentration in ARS (0.15 mM) and selected PBA (5 mM for PBA and o-AM-PBA) in PBS, and a range of concentration for the diol of interest that varied between diols due to their different affinities and that was adapted for each of the diol tested. A solution with ARS at 0.15 mM and without PBA and a solution ARS (0.15 mM) and PBA (5 mM) without diol of interest were used as reference for the following calculations. All the solutions were buffered to pH 7.4. To calculate the association constant of the PBA-diol complex, several equations were used as described below, from the new equilibrium induced

by the addition of the competitive diol. Based on mass-balance equations for the new equilibrium:

$$[ARS]_0 = [ARS] + [PBA - ARS] \quad \textbf{(8)}$$

$$[PBA]_0 = [PBA] + [PBA - ARS] + [PBA - diol] \quad \textbf{(9)}$$

$$[diol]_0 = [diol] + [PBA - diol] \quad \textbf{(10)}$$

And the association constant of the PBA-diol complex is defined as:

$$K_{eq} = \frac{[PBA - diol]}{[PBA][diol]} \quad \textbf{(11)}$$

From **(1), (8), (9), (10),** and **(11):**

$$[PBA]_0 = [PBA] + \frac{K_{eq}[PBA][diol]_0}{1 + K_{eq}[PBA]} + \frac{K_{ARS}[PBA][ARS]_0}{1 + K_{ARS}[PBA]} \quad \textbf{(12)}$$

From this equation, two variables were defined:

$$Q = \frac{[ARS]}{[PBA - ARS]} = \frac{A - A_{PBA-ARS}}{A_{ARS} - A} \quad \textbf{(13)}$$ for the absorbance measured at 530 nm

$$Q = \frac{[ARS]}{[PBA - ARS]} = \frac{A_{PBA-ARS} - A}{A - A_{ARS}} \quad \textbf{(13bis)}$$ for the absorbance measured at 450 nm

Where A is the absorbance of each sample of the range, $A_{PBA-ARS}$ is the absorbance of the PBA-ARS solution without competitive diol, and A_{ARS} the absorbance of the ARS solution without PBA and diol. Then, **(12)** can be written as:

$$[PBA]_0 = \frac{1}{Q.K_{ARS}} + \frac{K_{eq}.[diol]_0}{Q.K_{ARS} + K_{eq}} + \frac{[ARS]_0}{1 + Q} \quad \textbf{(14)}$$

P, the second variable is defined as:

$$P = [PBA]_0 - \frac{1}{Q.K_{ARS}} - \frac{[ARS]_0}{1 + Q} = \frac{K_{eq}[diol]_0}{Q.K_{ARS} + K_{eq}} \quad \textbf{(15)}$$

$$\frac{[diol]_0}{P} = \frac{K_{ARS}}{K_{eq}}.Q + 1 \quad \textbf{(16)}$$

From (16) and by using the linear regression of the absorbance results for the range of diol of interest selected, the plot of $\frac{[diol]_0}{P}$ in function of Q is obtained and its slope can be extracted. The K_{eq} is the result of the division of the K_{ARS} by the slope of this plot. We validated the method with the measurement of several association constants already described. We first calculated the association constant between phenylboronic acid (PBA) and ARS. Using an ARS solution at 0.15 mM and a range of PBA concentration between 2 and 7.5 mM, we obtained an association constant value of 1 582 M^{-1} (at 450 nm) 1 554 M^{-1} (at 530nm), that are very similar between the two wavelengths used and which is close to the 1 300 M^{-1} obtained by Springsteen and Wang.[3] These results were obtained from the following graphics:

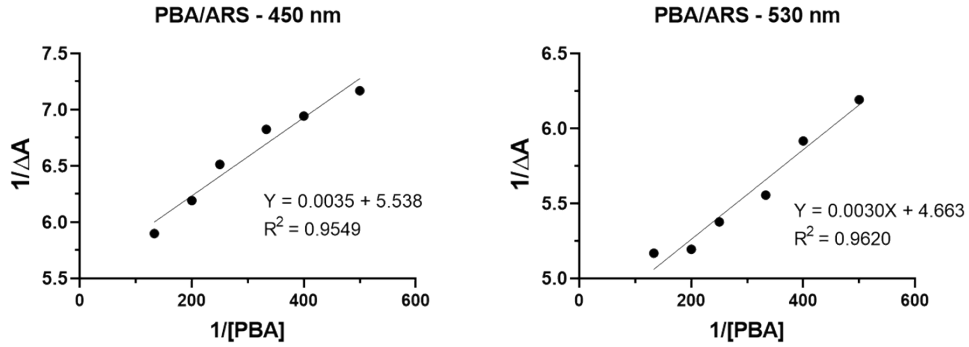

We then calculated the association constants between PBA and sorbitol as well as fructose. We used an ARS/PBA solution at 0.15 mM ARS and 5 mM PBA and a range of diol concentration between 7.5 and 100 mM for sorbitol and between 18.75 and 250 mM for fructose. We obtained an association constant value of 351 M^{-1} (at 450 nm) and 398 M^{-1} (at 530 nm) for PBA/Sorbitol and 208 M^{-1} (at 450 nm) and 176 M^{-1} (at 530 nm) for PBA/fructose. These results confirmed that comparable values are obtained using measurements at 450 nm or 530 nm, and that these are close to those obtained by Springsteen and Wang for the same pairs (370 M^{-1} and 160 M^{-1}, respectively).[3] These results were obtained from the following graphics:

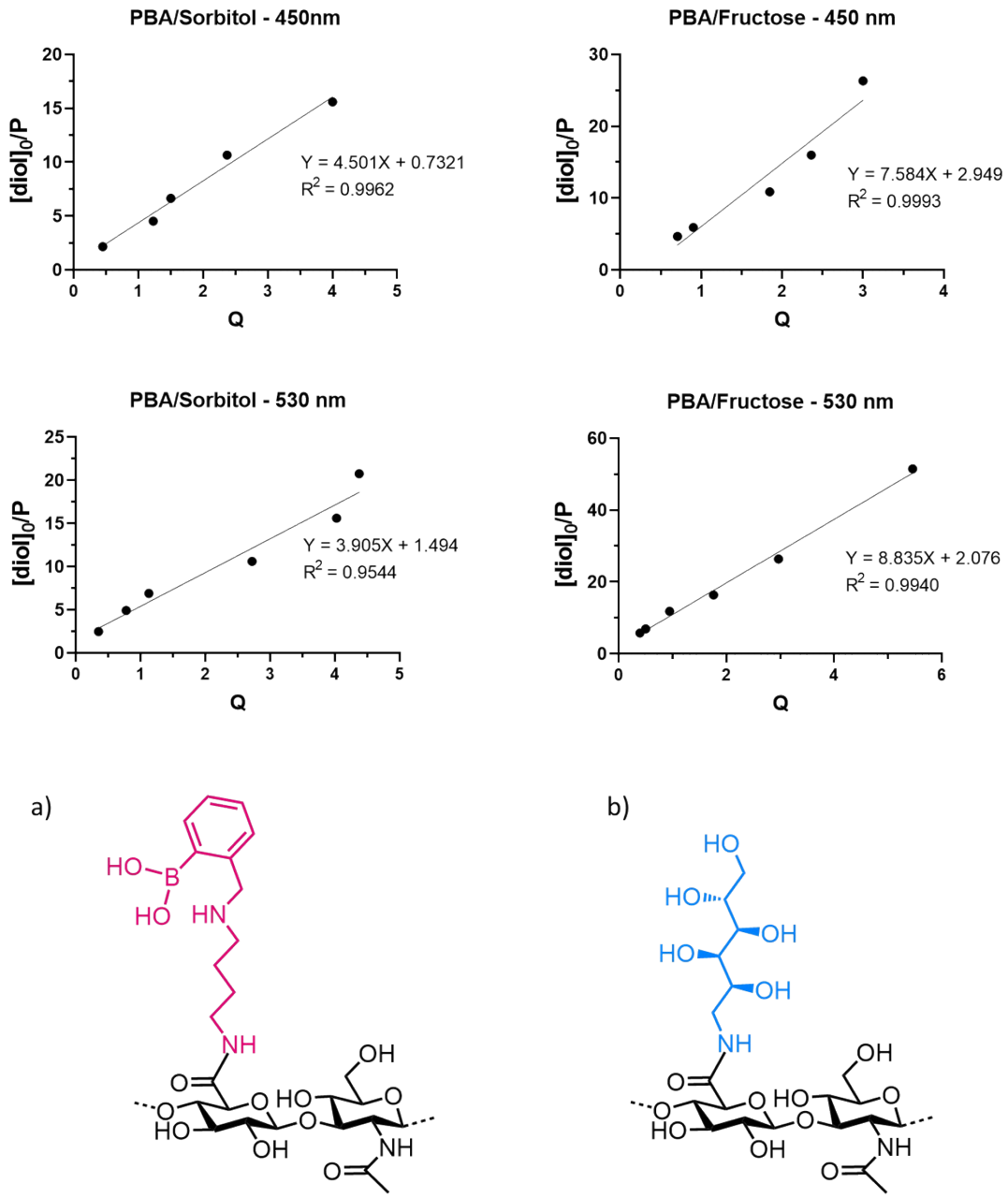

Figure S1. Structures of functionalized hyaluronic acid (HA) with a) *o*-AM-PBA and b) glucamine.

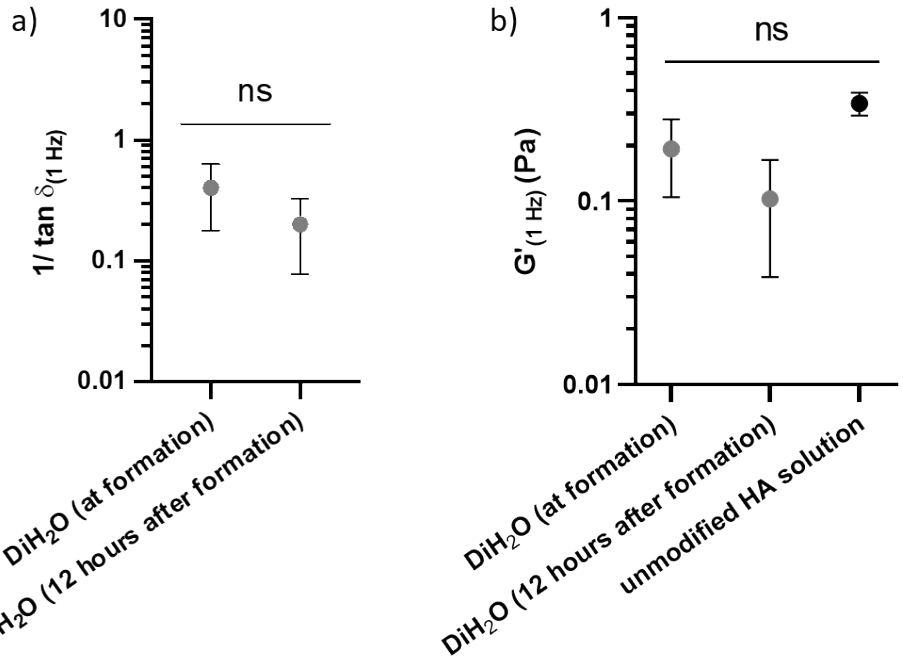

Figure S2. Rheological properties of the HA-*o*-AM-PBA/HA-glucamine mix in DI water at t_0 or after 12 hours of incubation at 37°C. a) 1/tan δ at 1 Hz ($1/\tan \delta_{(1\ Hz)}$) showed that the hydrogel is not formed in both conditions. b) G' at 1 Hz ($G'_{(1\ Hz)}$) values corroborate the first observation, the two conditions showed extremely low storage moduli, comparable to an unmodified HA solution at 1% (w/v).

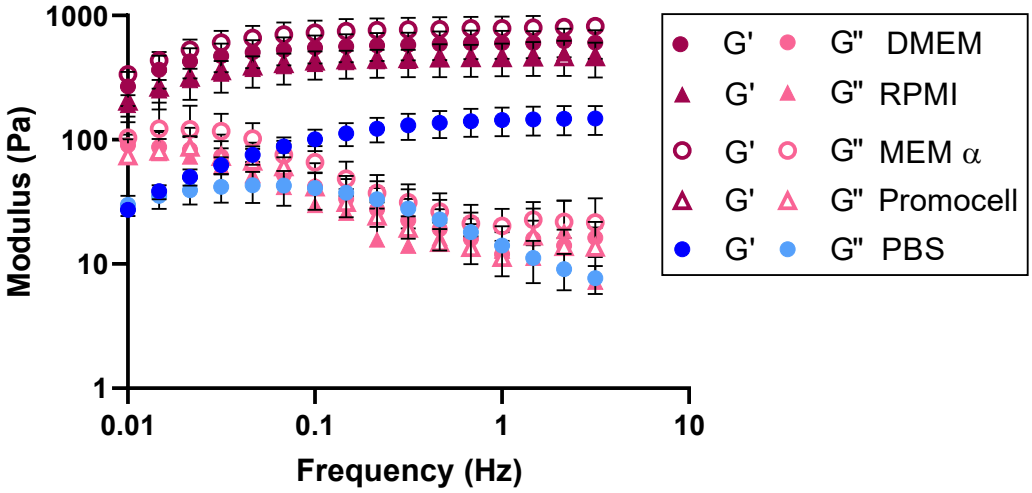

Figure S3. Frequency sweep measurements of HA-*o*-AM-PBA/HA-glucamine hydrogel in various media. We observe different rheological profiles between PBS and culture media, with a crossover frequency of 0.3 Hz for PBS compared to less than 0.01 Hz for the culture media.

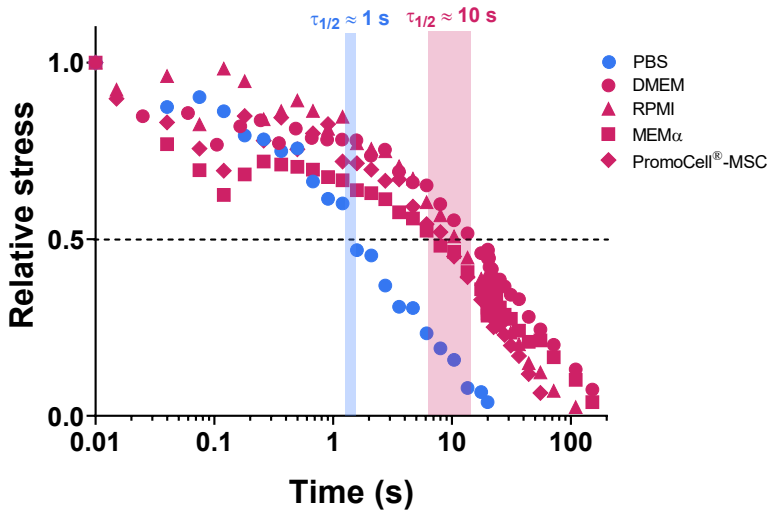

Figure S4. Stress relaxation measurements of HA-*o*-AM-PBA/HA-glucamine hydrogel in various media. We observed different stress relaxation profiles between PBS and culture media, with a half-relaxation time ($\tau_{1/2}$) of around 1 s for PBS compared to approximately 10 s for the culture media.

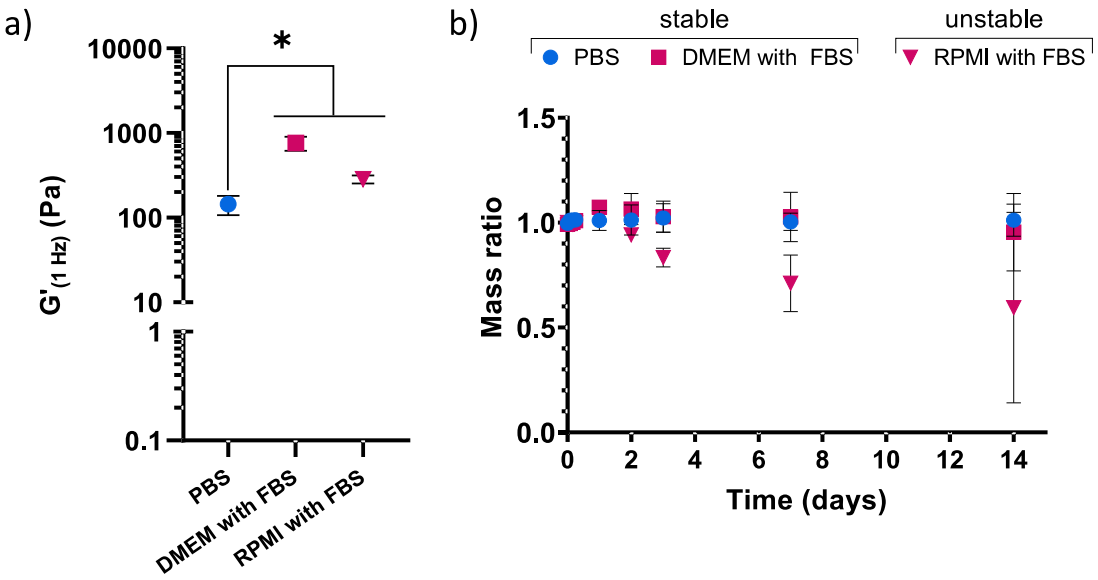

Figure S5. Effect of culture media with serum (FBS) on the physicochemical properties of the HA-*o*-AM-PBA/HA-glucamine hydrogel. a) Rheological property ($G'_{(1\ Hz)}$) of the same *o*-AM-PBA/glucamine hydrogel formulation were consistent with those made in the absence of FBS. b) Stability profile of the *o*-AM-PBA/glucamine hydrogel formulation in PBS, DMEM, and RPMI with FBS over 2 weeks showed a decrease in hydrogel mass of the hydrogel in RPMI

with FBS. Data are shown as mean ± SD (n = 3) with statistical significance determined using a t-test with Welch's correction (*p < 0.05).

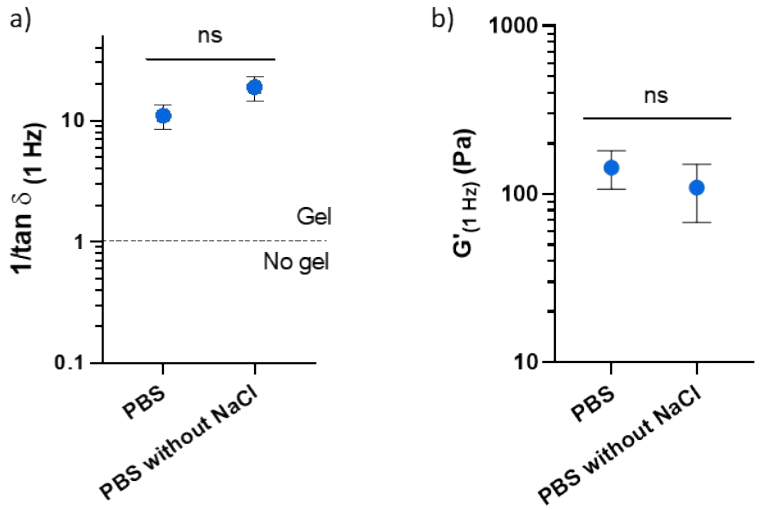

Figure S6. Rheological properties of the HA-*o*-AM-PBA/HA-glucamine hydrogel in PBS or PBS without NaCl (DI water with KH_2PO_4 [1 mM] and Na_2HPO_4 [3 mM]). a) 1/tan $\delta_{(1\ Hz)}$ showed that the hydrogel formed in both buffers. b) $G'_{(1\ Hz)}$ corroborates the first observation, the two conditions showed no significantly different modulus demonstrating that phosphate salts without NaCl are responsible for hydrogel formation.

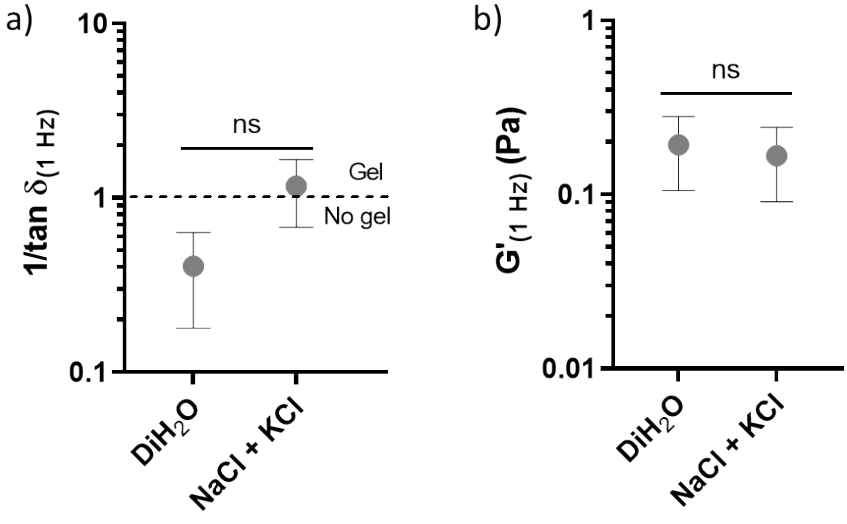

Figure S7. Effect of NaCl and KCl salts on the rheological properties of the HA-*o*-AM-PBA/HA-glucamine mix. a) 1/tan $\delta_{(1\ Hz)}$ showed no significant difference between the two conditions. b) $G'_{(1\ Hz)}$ values of the HA-*o*-AM-PBA/HA-glucamine mix in DI water

with or without 161 mM of NaCl and 1 mM of KCl (i.e., concentrations in DMEM) showed no significative change, with an extremely low $G'_{(1\ Hz)}$ in both conditions.

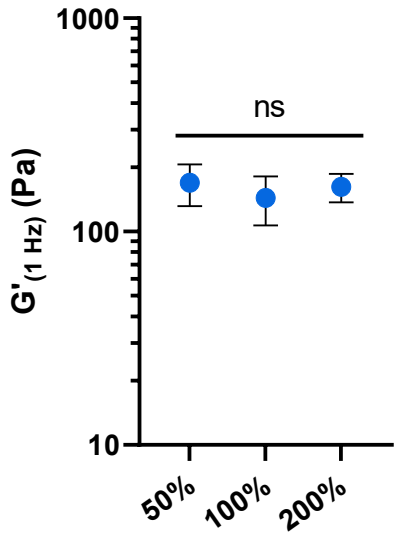

Figure S8. Effect of phosphate concentration on $G'_{(1\ Hz)}$ values with different buffers containing 50%, 100%, and 200% of the phosphate salts content of PBS. Doubling the phosphate concentration of PBS did not increase the $G'_{(1\ Hz)}$ value that reached a plateau at around 150 Pa.

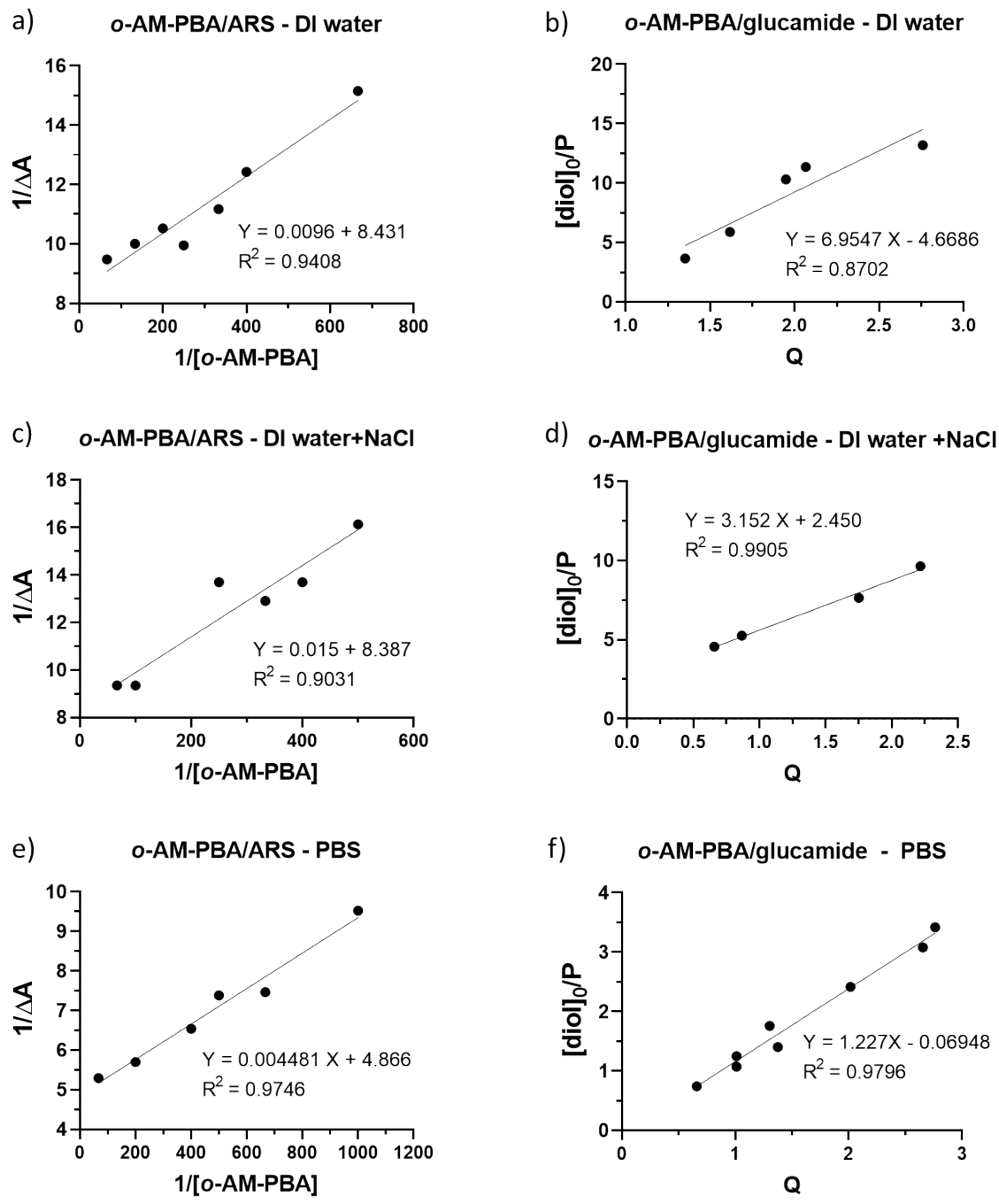

Figure S9. K_a calculation of *o*-AM-PBA/ARS and *o*-AM-PBA/glucamide in DI water, NaCl, and PBS, measured at 530 nm. a) K_a between *o*-AM-PBA (1-15 mM) and ARS measured in DI water, is equal to 878 M^{-1}. b) K_a between *o*-AM-PBA and glucamide (15–60 mM) measured in DI water is equal to 126 M^{-1}. c) K_a between *o*-AM-PBA and ARS measured in NaCl, is equal to 559 M^{-1}. d) K_a between *o*-AM-PBA and glucamide measured in NaCl is equal to 177 M^{-1}. e) K_a between *o*-AM-PBA and ARS measured in PBS, is equal to 1081 M^{-1}. f) K_a between *o*-AM-PBA and glucamide measured in PBS is equal to 881 M^{-1}.

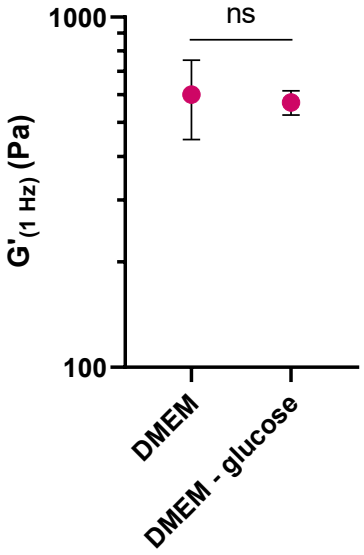

Figure S10. Effect of glucose on the rheological properties of the HA-*o*-AM-PBA/HA-glucamine hydrogel. Removing glucose from the DMEM culture medium had no impact on the $G'_{(1\ Hz)}$, then glucose is not responsible for the stiffening of BE hydrogels in culture medium.

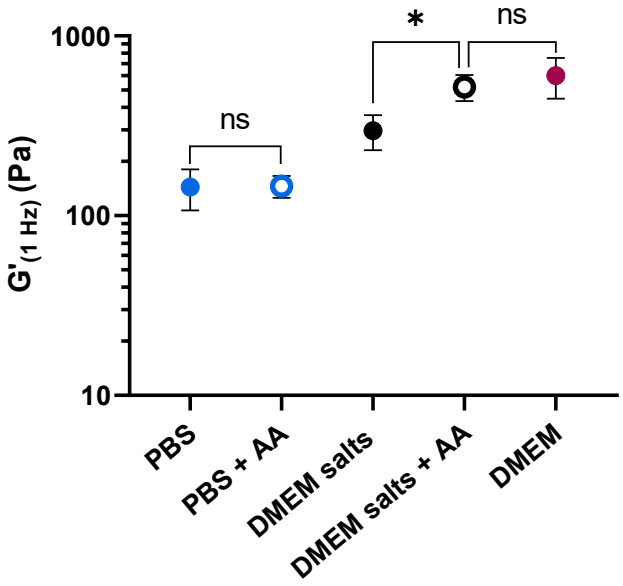

Figure S11. Effect of amino acids on the rheological properties of the HA-*o*-AM-PBA/HA-glucamine hydrogel. Adding amino acids to PBS had no impact on the $G'_{(1\ Hz)}$ value, whereas adding amino acids to DMEM salts induced an increase in $G'_{(1\ Hz)}$ value.

Data are shown as mean ± SD (n = 3) with statistical significance determined using a t-test with Welch's correction (ns = non significant, *p < 0.05).

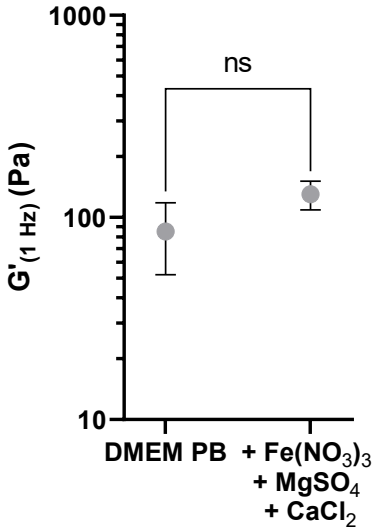

Figure S12. Effect of $Fe(NO_3)_3$, $MgSO_4$, and $CaCl_2$ salts on the rheological properties of the HA-*o*-AM-PBA/HA-glucamine hydrogel. The addition of these three salts to DMEM PB had no effect on the $G'_{(1\ Hz)}$.

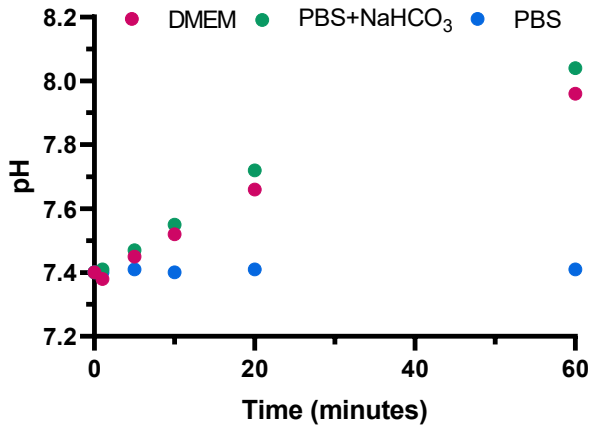

Figure S13. The pH of $PBS+NaHCO_3$ and DMEM (without phenol red) was not stable upon exposure to air and increased up to pH 8 after 1 hour.

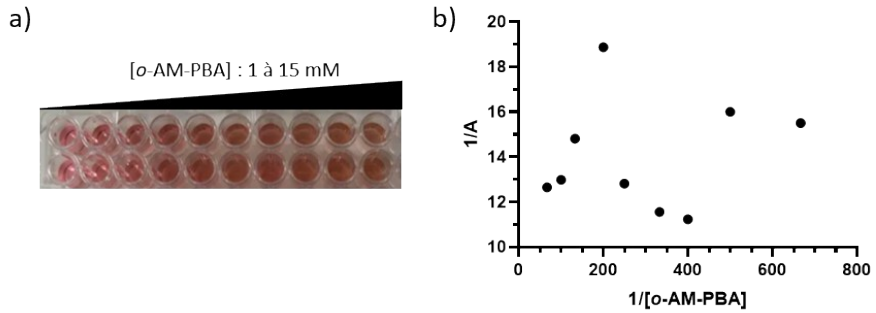

Figure S14. Association constant calculation for *o*-AM-PBA/ARS in PBS at pH 8. a) Picture of the samples showed few variations in color with the naked eye. b) 1/A vs 1/[*o*-AM-PBA] showed non-linear relationship prevented the calculation of the K_a of *o*-AM-PBA/ARS and *o*-AM-PBA/glucamide.

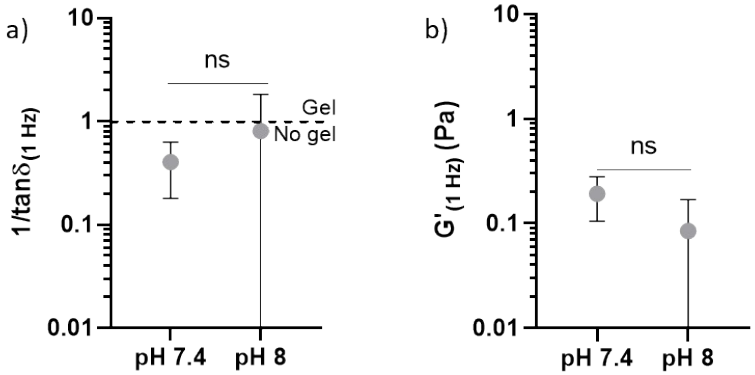

Figure S15. Effect of pH on rheological properties of the HA-*o*-AM-PBA/HA-glucamine mix in DI water. a) 1/tan $\delta_{(1\ Hz)}$ at pH 7.4 or 8 showed no significant difference. This hydrogel did not form in both conditions. b) $G'_{(1\ Hz)}$ of HA-*o*-AM-PBA/HA-glucamine mix. Increase in pH resulted in no significative change in $G'_{(1\ Hz)}$, which is very low in both conditions.

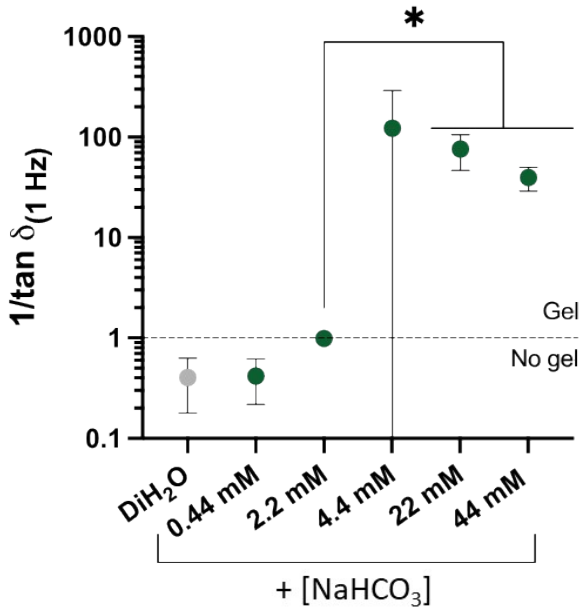

Figure S16. Evaluation of the 1/tan $\delta_{(1\ Hz)}$ of hydrogels formed in DI water with increasing concentration of $NaHCO_3$ showed hydrogel formation from 4.4 mM of $NaHCO_3$. Data are shown as mean ± SD (n = 3) with statistical significance determined using a t-test with Welch's correction (*p < 0.05).

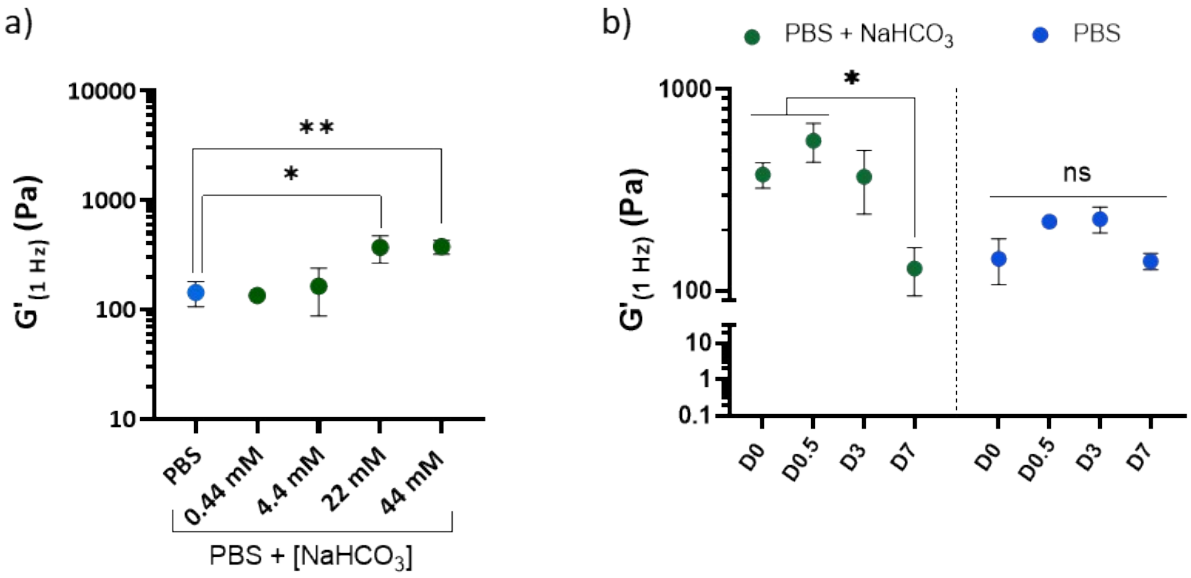

Figure S17. Evaluation of rheological properties with various concentration in $NaHCO_3$. a) Evaluation of rheological properties with various concentration in $NaHCO_3$ in PBS showed that $NaHCO_3$ induces an increase in $G'_{(1\ Hz)}$ value from 22 mM [$NaHCO_3$]. b) $G'_{(1\ Hz)}$ properties over time for three conditions (PBS, PBS + $NaHCO_3$, and DMEM) showed a transient effect of

$NaHCO_3$ on rheological properties. The impact of $NaHCO_3$ on rheological properties is negligible from day 7. Data are shown as mean ± SD (n = 3) with statistical significance determined using a t-test with Welch's correction (ns = non significant, *p < 0.05, **p < 0.01).

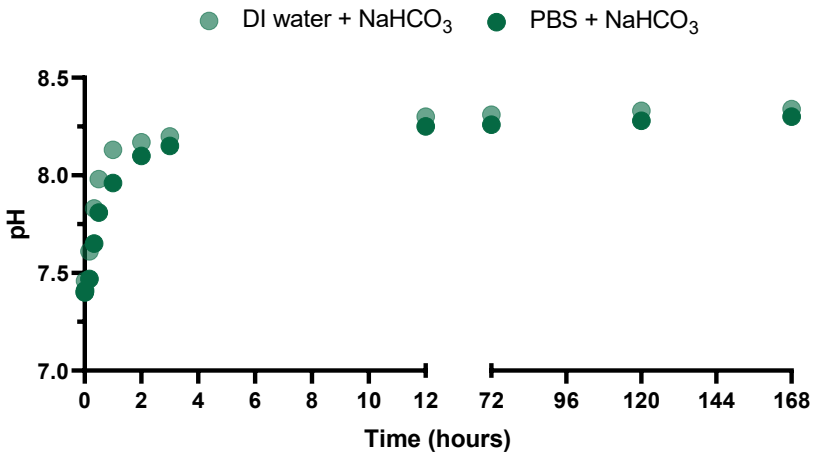

Figure S18. pH monitoring of DI water + $NaHCO_3$ and PBS + $NaHCO_3$ solutions over seven days. The pH of both solutions increased up to pH 8.3 after twelve hours before stabilizing for the next seven days.

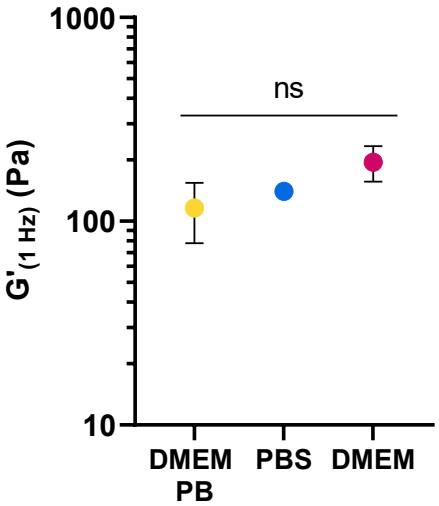

Figure S19. Evaluation of the $G'_{(1\ Hz)}$ of hydrogels formed in DMEM PB, PBS, and DMEM showed no significant difference after seven days of immersion in the buffer and media mentioned.

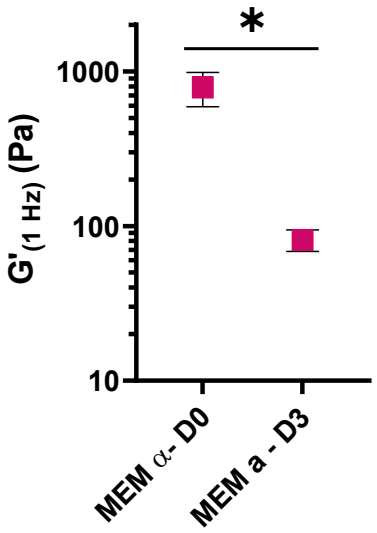

Figure S20. Evaluation of the $G'_{(1\ Hz)}$ of hydrogels formed in MEMα at D0 and after 3 days of immersion in MEMα. The transient properties are observed in MEMα as it was observed in DMEM. Data are shown as mean ± SD (n = 3) with statistical significance determined using a t-test with Welch's correction (*$p < 0.05$).

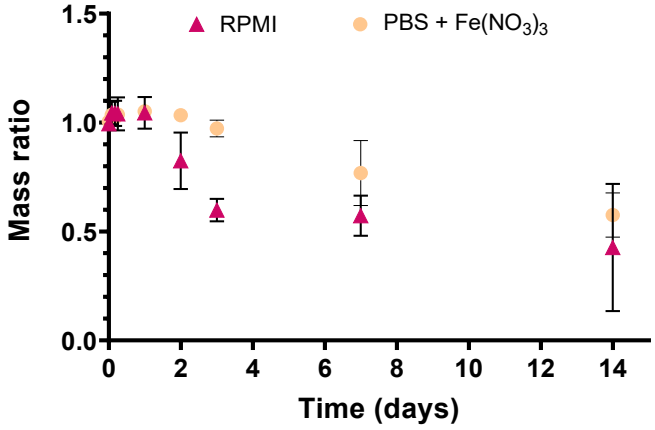

Figure S21. Swelling/stability profile of PBS + $Fe(NO_3)_3$ at 0.8 mM of NO_3^- ions showed similar stability profile as observed in RPMI and in PBS + $Ca(NO_3)_2$ therefore NO_3^- ions seems to be responsible for the hydrogel network degradation when associated with either Fe^{3+} or Ca^{2+}.

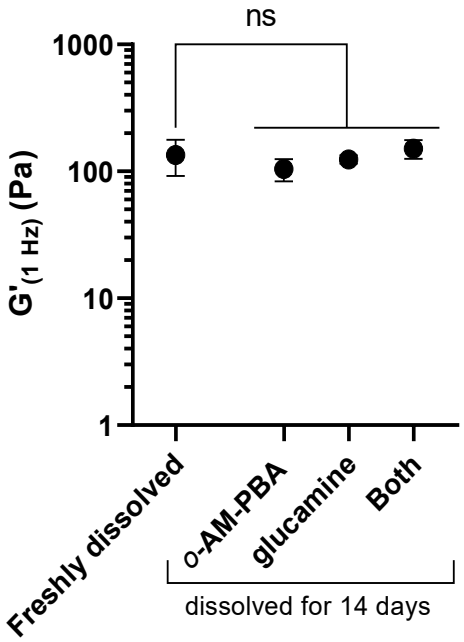

Figure S22. Rheological properties of *o*-AM-PBA/glucamine hydrogels with various dissolution time in $Ca(NO_3)_2$ of HA-*o*-AM-PBA and HA-glucamine prior to mixing and hydrogel formation. Fresh dissolution (overnight) or dissolution over 14 days for one of the two precursors or both did not have effect on hydrogel formation and rheological properties. After 14 days immersion with $Ca(NO_3)_2$ the precursors were not degraded.

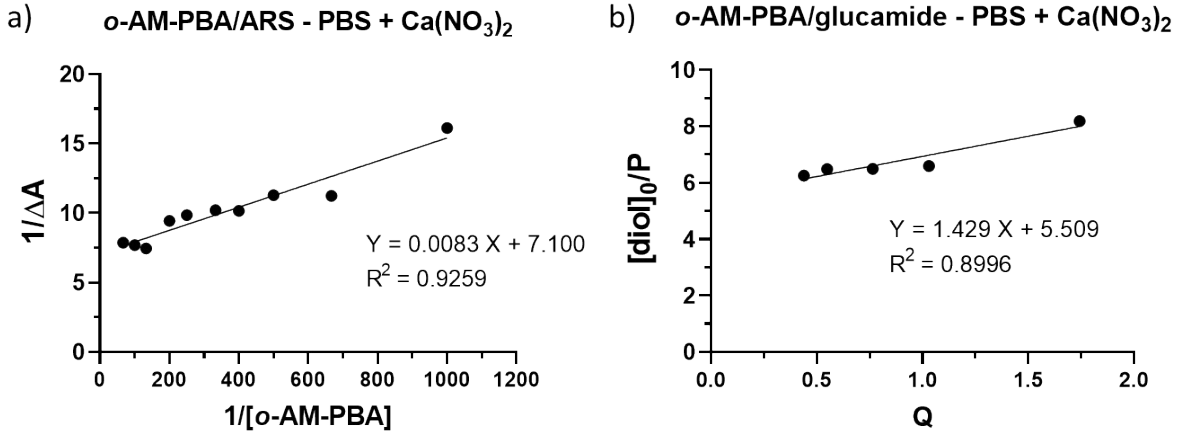

Figure S23. Calculation of the K_a of *o*-AM-PBA/glucamide pair in PBS with $Ca(NO_3)_2$. a) 1/ΔA versus 1/[PBA] for the determination of the K_a of the *o*-AM-PBA/ARS pair (0.15 mM ARS and [1-15 mM] *o*-AM-PBA), measured at 450 nm in PBS + $Ca(NO_3)_2$. The K_a is equal to 855 M^{-1}. b) $[diol]_0/P$ versus Q for the determination of the K_a of the *o*-AM-PBA/glucamide pair

(0.15 mM ARS, 5 mM *o*-AM-PBA and [14-22 mM] glucamide) measured at 450 nm in PBS + $Ca(NO_3)_2$. The K_a is equal to 598 M^{-1}.

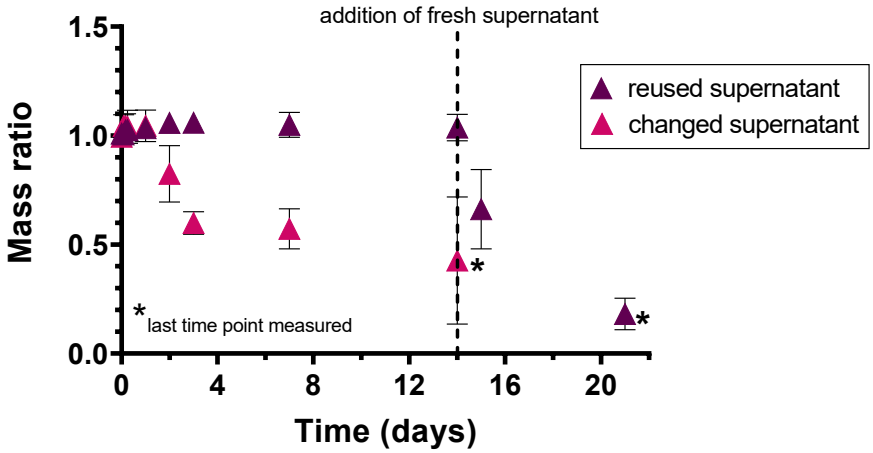

Figure S24. Stability/stability profile of hydrogels immersed in reused RPMI solution over 14 days or in a stock RPMI solution added at each time point showed that only the addition of stock RPMI induced a decrease in the mass of the hydrogels, as observed for PBS with $Ca(NO_3)_2$.

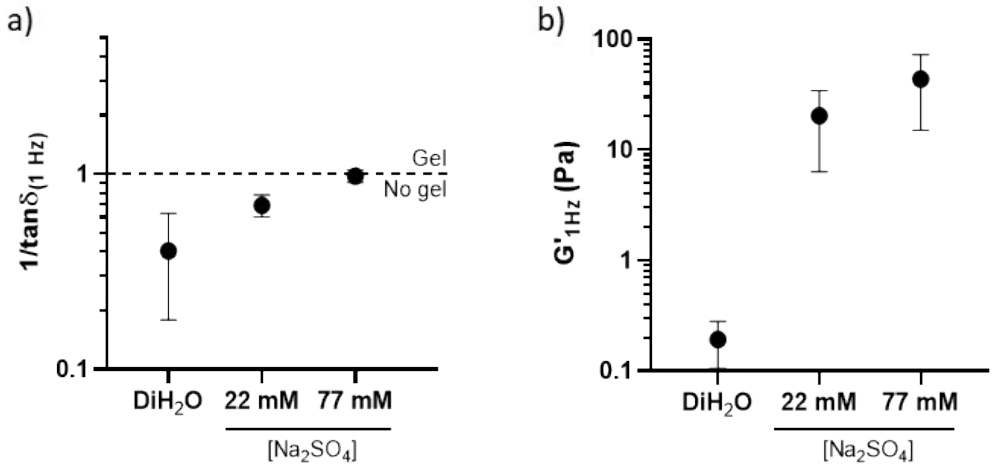

Figure S25. Effect of the addition of $NaSO_4$ to DI water on a) the hydrogel formation ($1/\tan \delta_{(1\ Hz)}$) and b) on the $G'_{(1\ Hz)}$ of HA-*o*-AM-PBA/HA-glucamine mix. Increase in $NaSO_4$ concentration induced hydrogel formation and an increase in $G'_{(1\ Hz)}$ values.

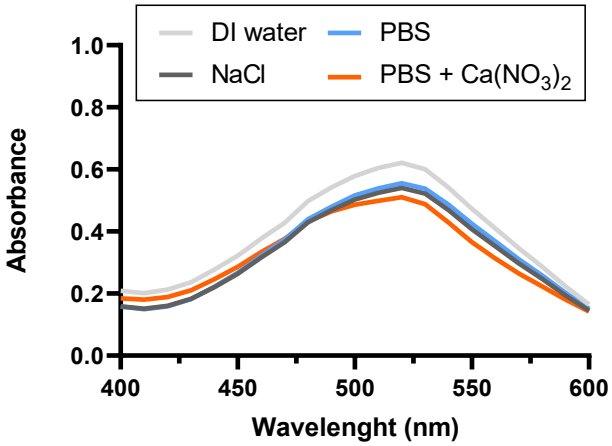

Figure S26. Evaluation of the effect of oxyanions on the ARS assay. Absorbance spectra of ARS in deionized (DI) water, NaCl (155 mM), PBS, and PBS with $Ca(NO_3)_2$ (0.4 mM).

References

1 M. Dowlut and D. G. Hall, *J Am Chem Soc*, 2006, 128, 4226–4227.

2 M. Bérubé, M. Dowlut and D. G. Hall, 2008, preprint, DOI: 10.1021/jo800788s.

3 G. Springsteen and B. Wang, *Tetrahedron*, 2002, 58, 5291–5300.